Journal of Biomechanics 50 (2017) 151–157

Contents lists available at ScienceDirect

Journal of Biomechanics

journal homepage: www.elsevier.com/locate/jbiomech
www.JBiomech.com

Quantitative T2 mapping for detection and quantification of thrombophlebitis in a rabbit model

Dar Weiss [a,*], Oren M. Rotman [b], Shmuel Einav [a,b]

[a] Department of Biomedical Engineering, Faculty of Engineering, Tel Aviv University, Tel Aviv 69978, Israel
[b] Department of Biomedical Engineering, Stony Brook University, Stony Brook, NY 11794, USA

ARTICLE INFO

Article history:
Accepted 2 November 2016

Keywords:
Edema
Inflammation
MRI
Peripheral catheter
Thrombophlebitis

ABSTRACT

Short peripheral catheter thrombophlebitis (SPCT), a sterile inflammation of the vein wall, is the most common complication associated with short peripheral catheters (SPCs) and affects up to 80% of hospitalized patients receiving IV therapy. Extensive research efforts have been devoted for improvement and optimization of the catheter material, but means for examination of any novel design are limited, inaccurate and require costly comprehensive pre-clinical and clinical trials. Therefore, there is a conclusive need for a reliable quantitative method for evaluation of SPCT, in particular for research purposes examining the thrombophlebitis-related symptoms of any novel catheter design. In this study, we developed for the first time a quantitative MRI based tool for evaluation of SPCT. The extent and severity of SPCT caused by two different commercially available SPCs with known predisposition for thrombophlebitis, were studied in a rabbit model. MRI analysis was consistent with the standardized pathology evaluation and showed remarkable difference in the percent of edema between the experimental groups. These differences were in line with previous studies and provide evidence that this type of analysis may be useful for future assessment of SPCT *in vivo*. As a non-invasive method, it may constitute a cost effective solution for examination of new catheters and other medical devices, thereby reducing the need for animal sacrifice.

1. Introduction

Short peripheral catheters (SPCs) are ubiquitous in today's healthcare environment, enabling effective and direct delivery of fluids and medications intravenously (Intravenous (IV)) (Dougherty et al., 2008). The most common complication associated with their use is short peripheral catheter thrombophlebitis (SPCT) – a generic term for a sterile inflammation of the vein wall, which affects up to 80% of hospitalized patients receiving IV therapy (Panadero et al., 2002). Extensive research efforts have been devoted for improvement and optimization of SPC's material properties, such as mechanical design and chemical composition. The Proprietary BD Vialon™ biomaterial (Becton, Dickinson and Company), for instance, enables longer SPC dwell times within the vein compared to FEP (Teflon) catheters (Maki and Ringer, 1991). The B. Braun Introcan Safety® Family (B. Braun medical Inc.) has unique needle tip design for easier catheter insertion, less tissue tearing and faster healing (Cantrell, 2012). Examination of any novel catheter design is normally associated with *in vitro* mechanical tests followed by preclinical and/or clinical trials.

In clinical studies and in practice, SPCT is usually diagnosed and evaluated using well established numerical qualitative scales (Jackson, 1998) which are based upon manifestation of pain and visual symptoms, and monitored by the clinical teams. The catheter site is graded between 0 and 5 (5 being most severe) as to the presence and severity of signs indicative of SPCT such as erythema, swelling and induration. Grade 2 often indicates on early stages of SPCT and requires catheter removal (Jackson, 1998). As scales are qualitative, they are inherently subjective and exposed to personal interpretation, and thus differences between evaluations or even cases of misdiagnosis are prone to occur. In addition, visual signs will not necessarily evolve or alternatively may only be visible at late stages and thus appropriate diagnosis and treatment is not implemented.

In preclinical studies, assessment of inflammation development is often based on histopathology analysis, which accounts to be the gold standard for SPCT evaluation. This analysis method requires the animal sacrifice after a predetermined period to enable organ resection. It therefore allows a quantitative SPCT assessment only at a single time point throughout its progression, which is the final stage, directly before animal sacrifice. Thus, the inflammation

* Corresponding author. Fax: +972 3 6409448.
E-mail address: darweiss@gmail.com (D. Weiss).

http://dx.doi.org/10.1016/j.jbiomech.2016.11.021
0021-9290/

development rate during catheter indwelling cannot be tracked, except by the qualitative scale mentioned before. Finally, examination of a new catheter will involve the sacrifice of dozens of animals, and enormous related costs. Hence, a novel quantitative technique for evaluation of SPCT development is needed to improve the safety and efficacy profile of any novel catheter design.

MRI is commonly used these days for inflammation detection in various cardiovascular diseases (Fredriksson et al., 2016; Phinikaridou et al., 2012). A particular MRI protocol, termed T2 mapping, was developed and widely used for measurement of the extent of edema in acute myocardial infarction (MI). It has been found to be robust and reliable in both preclinical and clinical studies (Ghugre et al., 2011; Park et al., 2013; Zia et al., 2012).

We hypothesized that SPCT could be detected and quantified using T2 mapping protocol as well. If proven correct, this method may be utilized as a quantitative non-invasive tool for evaluation of edema as a biomarker for SPCT development, and might be able to eliminate the need for histological evaluations and animal sacrifice. The current study examines the proposed MRI tool *ex vivo* in a rabbit model, and compares the extent of vascular inflammation caused by two different commercial catheters of known predisposition to SPCT. The results are compared to histopathology evaluation.

2. Methods

2.1. Animals

Five Female New-Zealand White rabbits (Harlan™, Jerusalem, Israel), weighting 2.5–3.4 Kg were examined in the study. The rabbits were delivered to Tel-Aviv University (TAU) Institutional Animal Care facility seven days before the study for acclimatization. They were housed in a well-ventilated, temperature (20–22 °C) and humidity regulated room with free access to diet and water. All procedures were performed in accordance with the approved guidelines set forth by the TAU ethical committee (Assurance # M-11-097), while all efforts were made to alleviate animals suffering.

2.2. Experimental procedures

Rabbits were anesthetized subcutaneously with 1.5 ml cocktail solution containing 50 mg/kg ketamine and 3 mg/kg xylazine. Rabbits' ears were then shaved and sterilized to facilitate SPC insertion and visualization of symptoms. Each ear was randomly assigned to one of the following treatment groups: naïve control (reference), and two different types of SPC (BD Insyte™) – 24 Gauge (G), 19 mm length or 20 G 30 mm length corresponding to outer cannula diameter of ~0.7 mm and ~1.1 mm, respectively (Fig. 1). Ears assignment to the different treatment groups is summarized in Table1. All catheters were inserted by an authorized veterinarian into the lateral aspect of the marginal ear vein, flushed with neutral saline (for vein patency test), and secured to the surrounding tissue with a designated transparent film dressing (Tegaderm™; 3 M). Following catheter securing, rabbits were dressed with Elizabethan collars (Vetmarket Ltd.) to prevent their access to the catheter site throughout the experiment. For the following 96 h, each catheter site was externally disinfected (alcohol 70% (w/v)) and its dressings were exchanged once a day. On the last study day (immediately prior to sacrifice), each rabbit ear was blindly evaluated by a trained veterinary technician for the presence of thrombophlebitis according to a clinical score (with modifications for rabbits) ranging from grade 0=no reaction to 4=severe inflammation (Levy et al., 1989). Rabbits were then subcutaneously sedated with a ketamine/xylazine mix solution (50 mg/kg and 3 mg/kg, respectively), and perfused with heparinized PBS through the main ear artery, to inhibit postmortem coagulation processes. Rabbits were euthanized by intra-cardiac injection of sodium pentobarbital, and immediately following sacrifice their ears (along with the catheters) were harvested and fixed in 10% buffered formalin (Santa Cruz biotechnology, Inc) for *ex vivo* MRI followed by histopathology.

2.3. Ex vivo MRI

At least 48 h prior to MRI acquisition, ears were washed repeatedly in PBS to remove formaldehyde remnants, and placed in a sterile PBS for rehydration. On the day of imaging, a rectangular-shaped section encompassing the catheterized vein region was excised from the entire ear tissue (Fig. 1) and embedded in Fluorinert liquid (3 M) to reduce susceptibility to artifacts. Care was taken to remove any residual PBS and air bubbles from each specimen. MRI was performed in a 30 cm-bore, 7 T MRI scanner (Bruker, Germany) having a maximal gradient strength of 400 mT/m and equipped with a designated four-channels surface coil. MRI protocol included T2 multi-shot multi-echo (MSME) sequence with the following parameters: 10 incrementing time echoes (10, 20, 30, 40, 50, 60, 70, 80, 90, 100 ms), repetition time (TR) =3500ms, pixel matrix size of 256 × 256 with an in plane resolution of 0.073 × 0.073 mm^2 (after reconstruction). For each specimen, images were obtained from 20 consecutive axial slices, while four acquisitions were averaged for each image and fat suppression was applied. Since there is a difference in the catheters length, for the 24 G catheter group images were acquired every

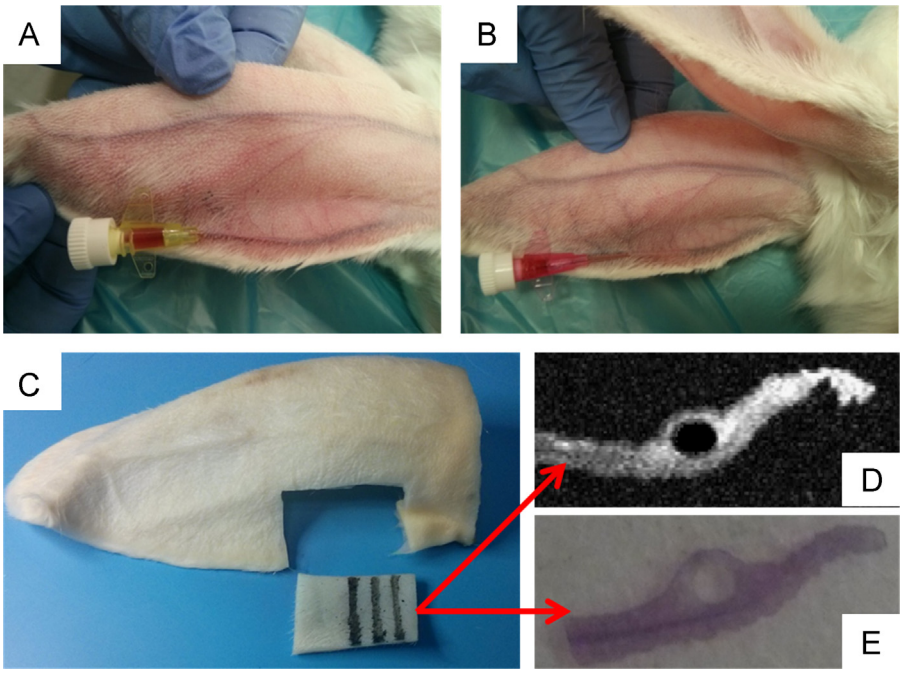

Fig. 1. Panels A and B correspond to ears catheterized with 24 G (yellow) and 20 G (pink) catheters. C. Example of the rectangular-shaped section which is excised from the entire ear tissue for MRI analysis (D) followed by histology (E). (For interpretation of the references to color in this figure legend, the reader is referred to the web version of this article.)

1 mm, whereas for the 20 G group images were obtained every 1.5 mm. Slice thickness was 300 μm for all specimens. The slices position was registered according to the catheter insertion site as a reference point, which was easily recognized in the images.

2.4. Image processing and analysis

For detection of the inflammation, MR images were analyzed to yield quantitative T2 maps, using bespoke software written in Matlab®(Matlab R2014a (8.3.0.532)). A non-linear least-squares algorithm was used to fit the MR signal to the non-negative, mono-exponential equation, in a voxel by voxel manner:

$$S(t) = S_0 * e^{-\left(\frac{TE}{T_2}\right)} \quad (1)$$

where $\boldsymbol{S}(t)$ denotes the vector of measured MR signal intensities (SI) for each voxel in the T2 weighted image, for each echo time (TE). S_0 and the T_2 relaxation time, extracted from the exponential decay, were derived for each voxel in each MRI cross section. Only TE that produced SI higher in ± 2 SD (standard deviation) than the mean noise value was considered for the exponential fit calculation per each voxel. Noise was determined in a region of interest (ROI) located outside of the specimen. The goodness of fit (GOF) was evaluated using R^2. Voxels whose GOF were smaller than 0.9 were excluded from the analysis. Evaluation of the proportion of inflamed area in each ear tissue was performed by constituting a Receiver Operating Characteristic (ROC) curve. The T2 values of control ears were defined as "normal" healthy voxels and ROC analysis was applied using several thresholds of T2 values ranging from 40 to 50 ms. Sensitivity and specificity were calculated for each threshold. Finally, each scanned slice was analyzed to produce percentage of total tissue edema according to the selected threshold in the following manner:

$$\%Edema = \frac{\#pixles\ above\ threshold}{\#total\ slice's\ pixels} \quad (2)$$

2.5. Histopathology evaluation

At the completion of the MRI experiment, each specimen was assigned a random identification number, re-fixed in 10% neutral-buffered formalin and sent for histopathology analysis done by a pathologist, blinded to the study conditions. The specimens were serially cross-sectioned, trimmed perpendicular to the marginal vein, embedded in paraffin, sectioned at 5 μm thickness and then stained with hematoxylin and eosin (H&E). For registration of MR images and histological sections, the venopuncture site and the gross morphology were used as references. We did not account for specimen shrinkage, as it can vary across specimens. The samples were evaluated and scored using semi-quantitative grading (Shackelford et al., 2002) accounting for the severity and/or extension of their response (0=none, 1=slight, 2=mild, 3=moderate, 4=severe). The parameters evaluated were Inflammatory infiltration degree, Edema, Denudation of endothelium and Thrombus formation.

2.6. Statistical analysis

All data are presented as mean ± standard error of the means (SEM)/standard deviation (SD). For pathological evaluation comparison (2-group comparisons) Multiple student's *t*-test were used whereas non-parametric Kruskal-Wallis test followed by Dunn post hoc test was used to detect differences in T2 values, on the T2 maps among the three experimental groups. Probability values of $P < 0.05$ were considered significant. Analyses were carried out using SPSS software, version22.01.

3. Results

A total number of ten ears (five rabbits), divided into three experimental groups, were studied for the extent and severity of edema using both T2 mapping analysis and histopathology. An example of obtained T2 maps (TE=10 ms) for a 24 G ear are illustrated in Fig. 2(A), where 13 out of 20 slices, separated by 0.7 mm inter-slice gap, are stacked in a 3D structure, visually demonstrating image registration. One representative 2D T2 map, for one slice (located distally to the catheter insertion site) is given in Fig. 2(B). Identification of tissue pixels as compared to the surrounding area, as well as classification to inflamed (high T2 value) versus healthy (low T2 value) tissue regions, can be easily recognized, providing evidence that this type of analysis may be useful for inflammation assessment.

A comparison between T2 values distribution, as demonstrated in the boxplot given in Fig. 3, reveals a significant difference between T2 values obtained for treated ears and control. The averaged T2 value for all slices of control ears was 39.7 ms ($p < 0.001$ vs. both catheter groups), while in the treated groups T2 values were found to be 48.01 ms and 53.9 ms for the 24 G and 20 G catheter ($p < 0.005$), respectively. Roc analysis set T2 value of 43 ms as the optimal threshold with the highest specificity and sensitivity. Threshold crossing was then used to classify each tissue pixel as healthy or inflamed, as depicted in Fig. 4. Such classification analysis was performed on each slice for each ear, yielding the percent edema per slice (Fig. 5(A)), and the total volumetric edema for the whole ear (Fig. 5(B)). As demonstrated in Fig. 5(A), the first two slices of both the 24 G and 20 G are characterized by similar inflamed area (± 35%). These slices are located at the venopuncture wound in the vein (catheters insertion site). The difference between both treated groups is more pronounced on the distal part of the veins, where the catheter and the vein's

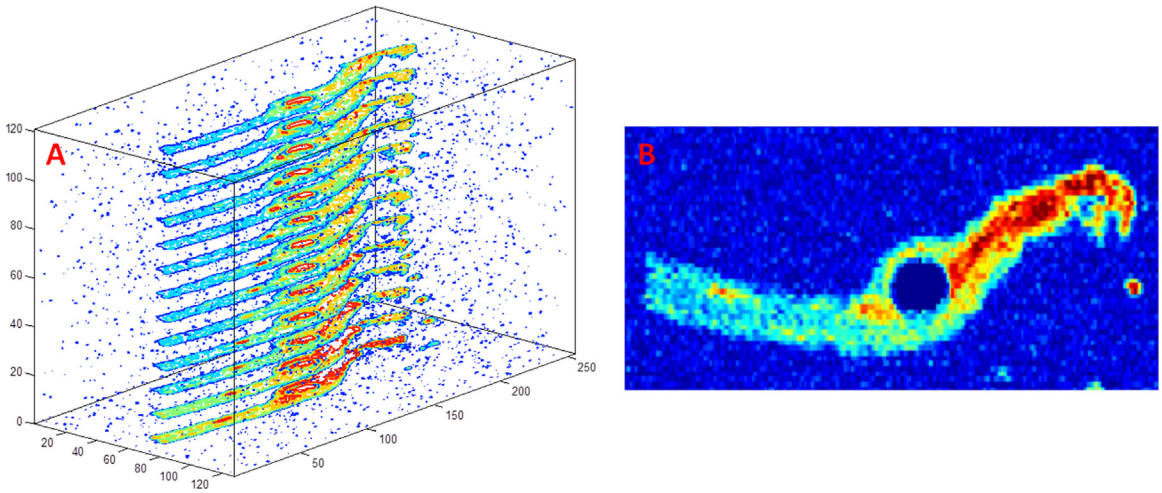

Fig. 2. (A) T2 maps obtained for different slices of 24 G catheterized ear, stacked in a 3D structure, demonstrating the ear's MRI acquisition procedure and the obtained T2 maps analysis results. (B) Two-dimensional saggital representation of the T2 map of one representative slice. Hot colors represent higher T2 values and vice versa. The blue hole inside the specimen indicates the location of the catheter. (For interpretation of the references to color in this figure legend, the reader is referred to the web version of this article.)

wall come into contact. With regard to the total edema volume described in Fig. 5(B), 74% of the total scanned tissue of the 20 G catheter group was classified as inflamed, while only about 46% was attributed to the 24 G group ($p=0.047$). Both catheter groups showed significantly higher edema rates compared to the control ($p<0.02$).

Histological findings suggested that the tissue surrounding the catheters of both treated groups developed marked edema which was more pronounced away from the puncture area. The edema appeared to be much more severe in the 20 G group. The presence of the 20 G catheter further caused severe stretching of the venous wall and exfoliation of the endothelial layer, where only ~20% of the wall (its upper part which is less exposed to the catheter) was lined with endothelium. Moderate multifocal heterophilic (rabbit's inflammatory cells) infiltration and marked lymphatic dilation were observed in the 20 G catheter group, while the presence of the 24 G catheter caused minimal mononuclear infiltration and only mild lymphatic dilation. All control veins were found to be within normal limits, with dermis without signs of inflammation, edema or lymphatic dilation. Fig. 6 summarizes the pathological findings for the evaluated parameters, and Fig. 7 shows the MRI derived images and the histological sections for representative vein cross sections. In contrast to the MRI and histology, the clinical visualization score failed to diagnose thrombophlebitis and differentiate between the experimental groups (Table 1). Only slight changes in the vein color were observed in some of the ears (3 out of 6 catheterized ears) and limited edema (1 mm area transversing the vein) appeared in one 20 G catheter.

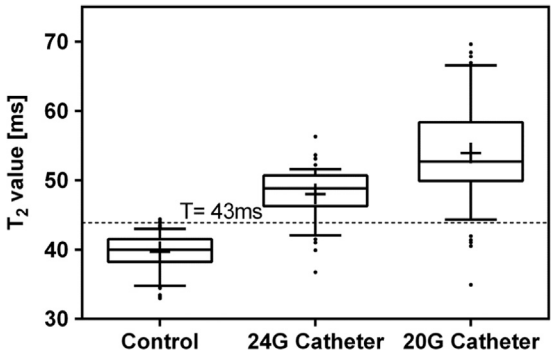

Fig. 3. Box plots demonstrating the T2 Value for the different groups. Each data sample represents an average of all the values within one slice. For each box the "+" sign denotes the average and the median is indentified by the line inside the box. The top and bottom of the box are the 25th and 75th percentiles of the samples, respectively. Outliers values are displayed with filled dots. Bars represent minimum and maximum (five numbers summary).

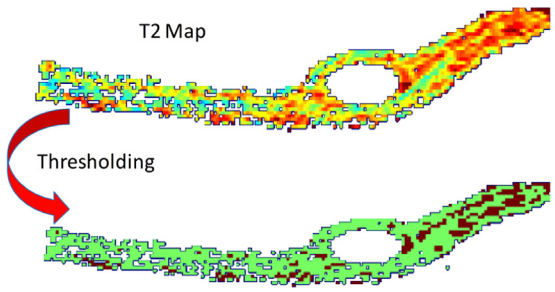

Fig. 4. Illustration of the threshold crossing procedure which was applied to each pixel in each slice, to obtain inflammatory classification. Upper panel shows the original T2 map, and lower panel describes the algorithm decision in which light green and dark red pixels stands for healthy and inflamed tissue pixels, respectively. (For interpretation of the references to color in this figure legend, the reader is referred to the web version of this article.)

4. Discussion

The severity and extent of edema as detected and quantified using the quantitative T2 mapping was in excellent agreement with the pathological evaluation. Our results show that characterization of SPCT can be accurately accomplished using *ex vivo* MRI.

SPCT results in pain, discomfort, and limitation to vascular access. More serious complications include purulent SPCT and sepsis which have subsequent effects on patient care quality and length of hospitalization (Ingram and Lavery, 2005). Non-well controlled SPCT may enhance the personal financial costs to patients and the medical cost expenditure of the hospitals. Although SPCT etiology is well-established and deemed to be multifactorial relating to biochemical, biomechanical, infection-related factors and patient-specific characteristics (Ahlqvist, 2010; Campbell, 1998; Macklin, 2003) its pathogenesis still remain unclear.

Recently, we demonstrated the importance of the biomechanical interaction between SPCs and the inner vein wall on the evolution of SPCT (Rotman et al., 2013; Weiss et al., 2016). The pressure exerted by the catheter irritates and activates the endothelium lining the wall thus promotes inflammation processes.

These findings led us to design a novel catheter configuration-Very Short Peripheral Catheter (VSPC) (Rotman and Einav, 2011) which eliminates the contact between the catheter and the vein

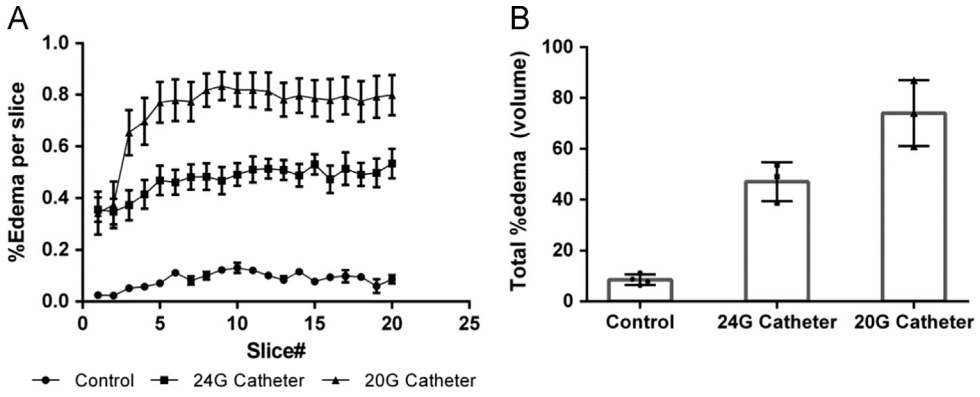

Fig. 5. A. The percent of edema (normalized to 0–1 range) per slice and the SEM (standard error of the means) bars which relates to the different specimens in each experimental group. 20 slices were produced for each specimen while Slice #1 corresponds to the catheter insertion site and slice#20 in each group fits to the most distal part in which the vein and catheter are still in contact. B. Volumetric percent of edema in each examined specimen presented as mean ± SD. Each dot describes one specimen (total of 10).

wall, thereby alleviating the stress acting upon the wall allowing relief of symptoms arising from SPCT.

To establish the priority of our novel catheter design, it was first required to establish a solid and sensitive method that enables to detect SPCT and reliably compare different severities. Several attempts to detect and quantify thrombophlebitis using thermography are reported in the literature (Ward et al., 1991a, 1991b). Thermography relies on the local temperature elevation, which is associated with the onset of the inflammatory response. However, it was only demonstrated that diagnosis using thermography is as good as the visual response score, which as pointed above is qualitative and prone to misdiagnosis. Comparison of the thermography results to histolopathology evaluation was not reported in any of these studies. Furthermore, a major drawback of this method is its considerably strong dependency on environmental conditions such as humidity and light intensity, as well as to patient specific characteristics as skin color, perspiration rate etc. (Diakides et al., 2012). Here we present for the first time a MRI-based tool for quantitative evaluation of SPCT extent and severity. MRI is utilized today as a clinical diagnostic tool, however, its high precision and high quality performances make it more applicable as a research tool to study physiology or validate other techniques.

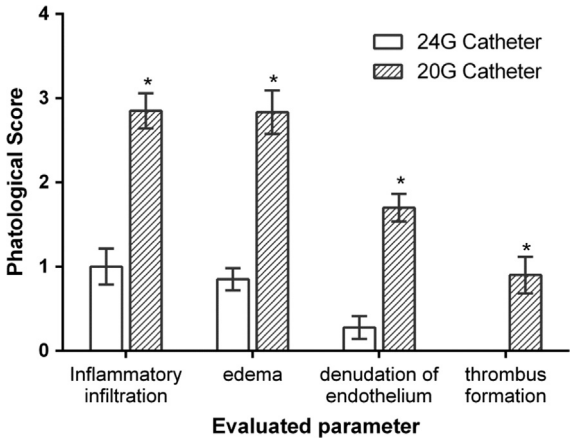

Fig. 6. Pathological evaluation. 20 histological slides (one section per slide) were derived for each ear specimen and each slide was graded between 0 and 4 (according to the semi-quantitative grading) with respect to one of the four evaluated parameters. The columns represent the average score for each catheter group. Control ears were not included in the graph as they were all graded "0". Bars stands for SEM ($*p < 0.001$).

The pioneering attempt to utilize MRI for quantification of SPCT described here was conducted using ex vivo *imaging*. Ex vivo imaging benefits from stronger field and greater resolution and sensitivity due to lack of constraints on imaging time and lack of motion artifacts. The goal at this preliminary stage was to compare the MRI results mainly to histopathology evaluation, which provide information only at a single time point before sacrifice. Thus, there was no need for precise time-course data, and in such case *ex vivo* imaging provides better results.

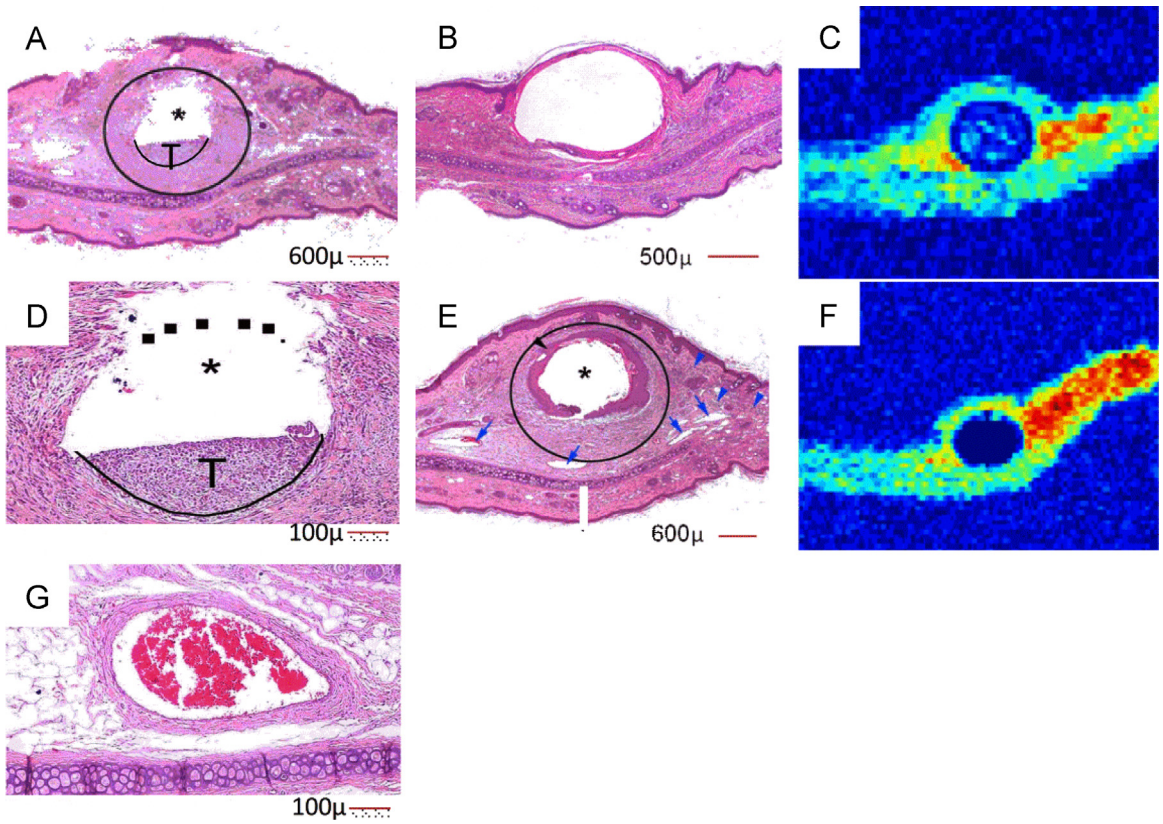

Fig. 7. Histopathology images (B+E) and the corresponding MRI (C+F) images of a rabbit marginal vein cross section. B+C panels represent the 24 G catheter group, while E+F describe the 20 G group. In panel E the venous lumen is marked with an asterisk, and multifocal mononuclear inflammation is labeled with blue arrowheads. Moderate dilation of large lymphatic vessels can also be observed (blue arrows). The circle around the vein indicates the approximate extent of tissue in which there is fibrosis. MRI images are T2-weighted (TE=20) with in-plane resolution of 73 μ. The MRI data was scaled to a specific colormap for display convenience. Panels A and D (magnification) describe a section of a 20 G catheter ear in which the vein has undergone thrombosis. The thrombus (T) is composed of loose fibrous tissue and occludes approximately one third of the lumen. The black line indicates the border between the loose venous wall and the thrombus. The circle in panel A indicates the approximate extent of the tissue surrounding the vein in which there is fibrosis and inflammation. The row of squares indicates the approximate level where the venous wall should be (based on consecutive sections). Panel G – section of a control vein, found to be within normal limits without any signs of inflammation. Red blood cells can be seen within the lumen. (For interpretation of the references to color in this figure legend, the reader is referred to the web version of this article.)

Table 1
Assignment of each rabbit ear to one of the treatment group: C-control (without catheter), 24 G and 20 G catheters. The bottom row depicts the clinical score as was evaluated prior to sacrifice.

Rabbit #	1		2		3		4		5	
Ear#	1L	1R	2L	2R	3L	3R	4L	4R	5L	5R
Treatment	20G	C	24G	C	20G	24G	20G	24G	C	C
Visual response score	1	0	0	0	2	1	0	0	0	0

Two different commercially available SPC with known predisposition for SPCT were selected for the study. It was previously shown that larger sized catheter diameter (corresponding to the 20 G catheter) causes greater damage to the vein and thus stimulates thrombophlebitis (Maki and Ringer, 1991). Given that, we hypothesized that in order to validate the quantification method using MRI, higher edema rate should be observed in the 20 G catheter group in comparison to the ones achieved for 24 G catheters and control. Indeed, higher edema volumes were obtained for the 20 G comparing to the 24 G and control (Fig. 5). These results were consistent with the pathology evaluation which confirmed that the MRI succeeded where the qualitative visualization grade failed.

The higher percent of edema obtained for the larger 20 G catheter (vs. 24 G catheter) were further consistent with our previous findings (Rotman et al., 2013; Weiss et al., 2016), suggesting that severity and development of SPCT may be strongly dependent on the contact pressure exerted by the SPCs on the vein wall. This is also manifested in Fig. 5(A) where it can be noticed that at the insertion site (Slice#1), edema percents are very similar, whereas distal to this point (Slice#3 and on), where the SPC and the veins wall mechanically interact and the wall constantly experience contact pressure, the difference is significant. It should also be noted that the 20 G catheter is longer than the 24 G one (30 mm vs. 20 mm), thus allowing wider contact area with the wall which probably also account for the difference between the obtained percent of edema.

The study findings coincide with clinical practice, which demonstrated that quantitative T2 mapping is a good objective technique for identifying and assessing the evolution of edema, and was further shown to be more robust than qualitative T2-weighted imaging (Park et al., 2013; van Heeswijk et al., 2012). Edema is the major symptom associated with the development of SPCT and is usually apparent in early stages following its onset. T2 values are related to the interstitial water content with higher values indicating on larger amount. The absolute water content, however, is not the only mechanism that can cause T2 changes. The movement of water molecules from the extracellular to the intracellular compartment as in pure cellular edema increases the T2 of the cytoplasm and nucleus (Knight et al., 1991) and has a stronger impact on T2 even in the absence of an increase in net water content (Hsu et al., 1996). This implies that edema is not necessarily accompanied by external visual signs and can be overlooked when diagnosed by visualization scale, however, can be detected using MRI.

The dispersion of the controls' T2 values found to be pretty narrow and low (Fig. 3) reflecting healthy-state structures comprising the ear tissue such as cartilage and fat. On the other hand, the catheter groups exhibited wider distribution with longer and abnormal relaxation times. These changes were the result of the edema (which was demonstrated in the pathology as lymphatic fluid accumulation) in the vicinity of the catheterized veins.

Beside the detection and quantification of SPCT which was described here, this technique could be useful in other applications which require assessment of extent and severity of inflammation. It can remarkably assist during development stages and characterization of any novel medical device by quantitative evaluation of its inflammation related risks. The method may further constitute a cost saving solution for testing new medical device by reducing the need for animal sacrifice.

The current study involved a small-scale trial and was therefore limited statistically. Moreover, a small animal model as the rabbit, forced us to work with relatively small veins, which limited the size choice of the SPCs. Future in vivo trials in a larger animal model are required to track the evolution of SPCT during the catheter dwelling period. Since this method (MRI) does not require animal sacrifice it will allow comparing the inflammatory response to our novel VSPC at several time points and not only at sacrifice. The main limitation of the method is the reliance on MRI which is still a very expensive tomographic modality. In addition, the quantification process of edema should be further calibrated in order to eliminate detection of edema in control specimens (Fig. 5). In the future, when the MRI will be more affordable and accessible it may suit clinical screening tests for SPCT, which will enable its early detection and thus improving quality of care.

Conflict of interest statement

The authors have no conflict of interests to disclose.

Acknowledgement

This study was partially supported by Joseph Drown Foundation (Grant no. 0605411342) and Herbert Berman Fund (Grant no. 0605534561).

References

Ahlqvist, M., 2010. Peripheral Venous Catheters – Quality of Care Assessment. Karolinska Institute.
Campbell, L., 1998. IV-related phlebitis, complications and length of hospital stay: 2. Br. J. Nurs. 7, 1364–1373.
Cantrell, S., 2012. Keeping IV infections out of site. Infect. Prev. 36, 16.
Diakides, M., Bronzino, J.D., Peterson, D.R., 2012. Medical Infrared Imaging: Principles and Practices. CRC Press.
Dougherty, L., Dougherty, L., Lamb, J., 2008. Obtaining Peripheral Venous Access. Blackwell Publishing, Oxford.
Fredriksson, A.G., Svalbring, E., Eriksson, J., Dyverfeldt, P., Alehagen, U., Engvall, J., Ebbers, T., Carlhäll, C.J., 2016. 4D flow MRI can detect subtle right ventricular dysfunction in primary left ventricular disease. J. Magn. Reson. Imaging 43, 558–565.
Ghugre, N.R., Ramanan, V., Pop, M., Yang, Y., Barry, J., Qiang, B., Connelly, K.A., Dick, A.J., Wright, G.A., 2011. Quantitative tracking of edema, hemorrhage, and microvascular obstruction in subacute myocardial infarction in a porcine model by MRI. Magn. Reson. Med. 66, 1129–1141.
Hsu, E.W., Aiken, N.R., Blackband, S.J., 1996. Nuclear magnetic resonance microscopy of single neurons under hypotonic perturbation. Am. J. Physiol. Cell Physiol. 271, C1895–C1900.
Ingram, P., Lavery, I., 2005. Peripheral Intravenous Therapy: Key Risks and Implications for Practice, 1987. Nursing standard (Royal College of Nursing, Great Britain, p. 55.
Jackson, A., 1998. Infection control – a battle in vein: infusion phlebitis. Nursing 94 (68), 71.
Knight, R., Ordidge, R., Helpern, J., Chopp, M., Rodolosi, L., Peck, D., 1991. Temporal evolution of ischemic damage in rat brain measured by proton nuclear magnetic resonance imaging. Stroke 22, 802–808.
Levy, M.Y., Langerman, L., Gottschalk-Sabag, S., Benita, S., 1989. Side-effect evaluation of a new diazepam formulation: venous sequela reduction following intravenous (iv) injection of a diazepam emulsion in rabbits. Pharm. Res. 6, 510–516.
Macklin, D., 2003. Phlebitis: a painful complication of peripheral IV catheterization that may be prevented. AJN Am. J. Nurs. 103, 55–60.
Maki, D.G., Ringer, M., 1991. Risk factors for infusion-related phlebitis with small peripheral venous catheters: a randomized controlled trial. Ann. Intern. Med. 114, 845–854.

Panadero, A., Iohom, G., Taj, J., Mackay, N., Shorten, G., 2002. A dedicated intravenous cannula for postoperative use effect on incidence and severity of phlebitis. Anaesthesia 57, 921–925.
Park, C.H., Choi, E.-Y., Kwon, H.M., Hong, B.K., Lee, B.K., Yoon, Y.W., Min, P.-K., Greiser, A., Paek, M.Y., Yu, W., 2013. Quantitative T2 mapping for detecting myocardial edema after reperfusion of myocardial infarction: validation and comparison with T2-weighted images. Int. J. Cardiovasc. imaging 29, 65–72.
Phinikaridou, A., Qiao, Y., Giordano, N., Hamilton, J.A., 2012. Detection of thrombus size and protein content by ex vivo magnetization transfer and diffusion weighted MRI. J. Cardiovasc. Magn. Reson. 14, 1.
Rotman, O., Einav, S., 2011. Catheter cannula with anchoring elements, catheter including thereof, and/or catheterization method using WO 2012007944 A1.
Rotman, O.M., Shav, D., Raz, S., Zaretsky, U., Einav, S., 2013. Biomechanical aspects of catheter-related thrombophlebitis. J. Biomed. Sci. Eng. 6, 6.
Shackelford, C., Long, G., Wolf, J., Okerberg, C., Herbert, R., 2002. Qualitative and quantitative analysis of nonneoplastic lesions in toxicology studies. Toxicol. Pathol. 30, 93–96.
van Heeswijk, R.B., Feliciano, H., Bongard, C., Bonanno, G., Coppo, S., Lauriers, N., Locca, D., Schwitter, J., Stuber, M., 2012. Free-breathing 3 T magnetic resonance T2-mapping of the heart. JACC: Cardiovasc. Imaging 5, 1231–1239.
Ward, G.H., Nolan Jr, P.E., Chawla, M., Yalkowsky, S.H., 1991a. Studies in phlebitis: detection and quantitation using a thermographic camera. Pharm. Res. 8, 76–79.
Ward, G.H., Nolan, P.E., White, M., Yalkowsky, S.H., 1991b. Studies in phlebitis. II. Early detection of amiodarone-induced phlebitis in a rabbit model. Pharm. Res. 8, 801–803.
Weiss, D., Gefen, A., Einav, S., 2016. Modelling catheter-vein biomechanical interactions during an intravenous procedure. Comput. Methods Biomechan. Biomed. Eng. 19, 330–339.
Zia, M.I., Ghugre, N.R., Connelly, K.A., Strauss, B.H., Sparkes, J.D., Dick, A.J., Wright, G. A., 2012. Characterizing myocardial edema and hemorrhage using quantitative T2 and T2* mapping at multiple time intervals post ST-segment elevation myocardial infarction. Circ.: Cardiovasc. Imaging 5, 566–572.